

Explainable AI for engineering design: A unified approach of systems engineering and component-based deep learning¹

Philipp Geyer^{2 3}, Manav Mahan Singh⁴, Xia Chen³

Abstract—Data-driven models created by machine learning gain in importance in all fields of design and engineering. They have high potential to assist decision-makers in creating novel artefacts with a better performance and sustainability. However, limited generalization and the black-box nature of these models induce limited explainability and reusability. These drawbacks provide significant barriers retarding adoption in engineering design. To overcome this situation, we propose a component-based approach to create partial component models by machine learning (ML). This component-based approach aligns deep learning to systems engineering (SE). By means of the example of energy efficient building design, we first demonstrate generalization of the component-based method by accurately predicting the performance of designs with random structure different from training data. Second, we illustrate explainability by local sampling, sensitivity information and rules derived from low-depth decision trees and by evaluating this information from an engineering design perspective. The key for explainability is that activations at interfaces between the components are interpretable engineering quantities. In this way, the hierarchical component system forms a deep neural network (DNN) that directly integrates information for engineering explainability. The large range of possible configurations in composing components allows the examination of novel unseen design cases with understandable data-driven models. The matching of parameter ranges of components by similar probability distribution produces reusable, well-generalizing, and trustworthy models. The approach adapts the model structure to engineering methods of systems engineering and to domain knowledge.

Index Terms—Artificial intelligence, machine learning, metamodelling, regression model, systems engineering, complex systems

I. INTRODUCTION

Increasingly data models provide assistance in complex engineering design tasks. The data models are meanwhile able to capture the complexities sufficiently and the computational power required to create the models is not a limiting factor anymore. Due to this reason, there are many applications in engineering-related domains, at least on the part of research. Many applications predict the energy demand of buildings [1]–[3] because it avoids complex modelling and high computational load required for simulations. Basically, these data models are used as surrogates for simulations in sustainable building design [4]. Learning methods serve to develop such surrogates, also called metamodels [1], [5]. Following the same pattern, surrogate data models for structural design and engineering have been created [6]. For dynamical systems, extreme learning with reduced training efforts has been established [7]–[9]. In fluid dynamics, data-driven modelling have been established for prediction of flows [10]. Methods of data-driven modelling and analysis have been applied in life sciences and health care [11]

¹ This work has been submitted to an IEEE journal for potential publication. Copyright may be transferred without notice, after which this version may no longer be accessible. This version has been created on 05 January 2022

² Sustainable Building Systems, Leibniz University Hannover, geyer@iek.uni-hannover.de

³ Digital Architecture and Sustainability, TU Berlin, Germany

⁴ Architectural Engineering, KU Leuven, Belgium

as well as in agriculture [12] with the objective to transform data into knowledge. Furthermore, in operations research and systems engineering for control and decision problems including the analysis of dynamic systems deep learning methods got attention, recently [13].

The scheme of data-driven modelling and analysis is similar in many applications. Valid simulation approaches exist. However, designers and engineers need feedback in real-time in a process called design space exploration (DSE), e.g. in energy-efficient building design, to understand how to improve a design configuration and to develop well-performing solutions [14]. This exploration process includes variation of a design configuration as a key technique to answer what-if questions. As this process requires analysis of many variants to gain this information, the use of physical simulations causes significant modelling and computation load. This load is a substantial load of real-time application in case physical simulation is used, which vitally limits the exploration process. However, not only designing requires evaluation of many variants and states but also building energy classification, clustering and retrofit strategy development [15], [16] as well as control and management problems [17]–[19]. In this situation, data-driven modelling trained either on simulation results or on data collected from existing artefacts are a highly interesting alternative to physical simulations.

However, there are two major limitations of current data-driven approaches for their use in engineering design. First, often in design and engineering, prediction models are applied to non-existing cases before production or construction. Therefore, decision makers need to be sure that models predict correctly in unseen cases different from the training data, which calls for a good generalization. Second, designers and engineers need insights in how the models predict to check and approve results as well as to gain understanding of the behavior of the design configuration and the nature of the design space. This situation calls for explainability of data-driven models.

To address the shortcomings of the black-box character of ML models, a lot of research is carried out addressing the latter by developing the methods for *explainability* [20]. On the one hand, they identify a limited set of transparent models that are interpretable by humans. On the other hand, a huge set of post-hoc methods add explainability to ML black-box models. The objective is to equip the models with a property called explainability, which makes them accessible to human interpretation. Human *interpretation* is possible if features, activations, and outcomes used in these models relate to those that have meaning in the respective domain. By this meaning, a process of *understanding* is enabled in that internal information is put in the context of the domain, relations to other domain information are drawn and plausibility and justification of models in a broader network of domain knowledge is generated. Accessing this information in a conventional DNN generated for the prediction without the component-based approach requires a relative high effort and is limited [21].

The other limitation of the data-driven models to be overcome is the one of generalization. These models are bound to the structure of training data and to the range these data cover because data-driven models have very limited capabilities of extrapolation. From these characteristics, there are two conditions of applicability. First, the models need to match the structure of inputs and outputs defined by training data. Second, for reliable prediction, the range and coverage of training data need to match. In design, novel cases frequently have different structures. This difference limits the traditional approach, which we call parametric monolithic modelling, significantly as it can only predict for design variations with relatively limited modifications covered by parametric changes. A workaround is the use of characteristic numbers with engineering meaning instead of the direct use of parameters. In energy performance prediction, the compactness, i.e. ratio of façade area to building volume, is such a number that replaces detailed geometric parameters and leads to good predictions of energy demand for a high variety of building designs [22]. This way of feature engineering provides some flexibility allowing for an extension of generalization. However, internal processes and specific design configurations are still not considered by these monolithic models. This fact limits both, generalization as model structures cannot be adapted and explainability as internal parameter information is not available.

In the next section, we introduce the approach of component-based ML to extend generalization. On this basis, section three shows how information at component interface enables direct explainability and how additional local analysis and models make further information on design space and the design's behavior available. The last two sections discuss the component-based approach and its results in a broader context and provide the details of the examples. For illustration, we use energy-efficient building

design and the respective necessary engineering and simulation of dynamic thermal and energy-related processes in the paper. This application forms a demonstration case with relative high systems complexity.

II. COMPONENT-BASED MACHINE LEARNING (CBML)

To improve both the generalizability and explainability, we propose a component-based approach that aligns data-driven modelling to design and engineering. We create data-driven models for the design and engineering process following a system engineering paradigm [23]. The decomposition according to this paradigm using system components with input and output parameters forming the interfaces between the components are the key elements of component-based ML. This approach provides the basis for engineering interpretability and the reusability of components leading to generalization. Furthermore, it makes the data-driven models accessible to existing systems analysis methods [24].

As the first step, a data-driven model for the component's behavior is trained by representative data of its context. Training data in this context can be real data collected from real world [25] or synthetic data generated by a state-of-the-art dynamic simulation tool [26], [27]. Training takes place in a supervised process component by component using the respective input and output data, as shown for windows and wall component in Figure 1a. In case of prediction, the components are composed to represent the design artefact in its current configuration. By connecting inputs and outputs of the components to a system representing new designs, the data models are reused for unseen configurations (Figure 1b). Aligning the component structure to the methods of digital modelling (in case of buildings: building information modelling, BIM [28]; industry foundation classes, IFC [29]) fosters automatic generation of the data models.

This approach based on systems engineering and components provides a much wider generalization than the monolithic approach. The approach is flexible and allows to meet the two criteria of applicability of data-driven models mentioned in the first section. First, the structure of data is met by selecting and composing the data-driven models as required to represent the design configuration. In the example, the monolithic model based on the training data shown in Figure 1a would only allow prediction for box buildings because of the structure of data and the model; the component-based approach allows prediction for a broad variety of design cases exemplified by the configurations shown in Figure 2, top. Because components occur in similar configuration in the novel design cases as they are present in the training dataset, the second condition of matching parameter value distributions is also met. The grey boxes in Figure 1 (c-h) show examples of the matching of parameter ranges. There are parameter ranges, such as the U value, which determines heat transmission through walls and windows, that can be configured directly and, thus, a perfect match is possible (Fig. 1d). Many other parameters depend on previously determined parameters for that no direct control is possible, but the match depends on other parameters of the design configuration. For instance, the wall area (Fig. 1c) depends on the building shape; heating and cooling loads (Fig. 1f,g) and the final energy demand (Fig. 1h) depend on dynamic thermal processes determined by component heat flows of the building envelope and zones parameters. Therefore, only an approximate match is achievable. The data show a very good match for the example although the configuration of training and prediction is significantly different. By complying with these two preconditions for use of data-driven models and by representing the design configuration by a data-model composition, the component-based approach delivers a good generalization with high flexibility.

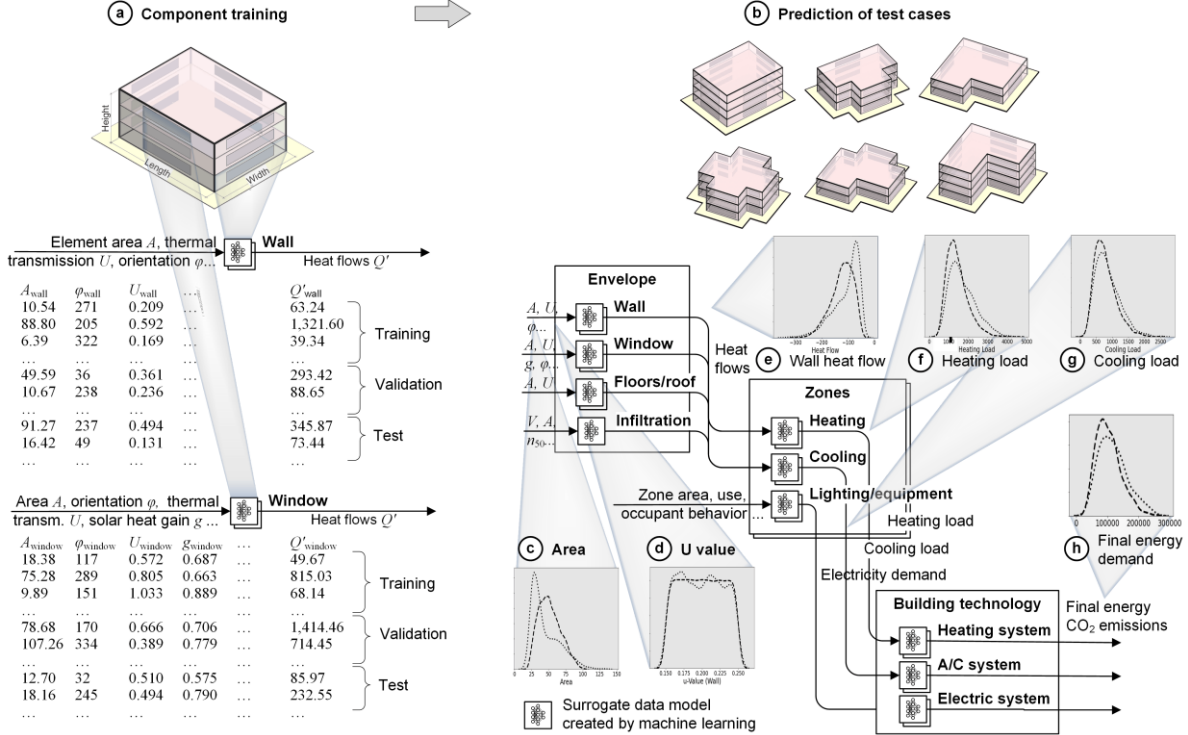


Fig. 1. Component-based machine learning (CBML). (a) Training takes place at component level. (b) For prediction of new cases, components are composed according to the structure of the new design. This allows representing novel unseen configurations. At the same time, it enables matching range and probability distribution of training data shown for exemplary parameters in the grey boxes (light dotted line: training data; thick dashed line: test data).

To examine the generalization capabilities, ML predictions have been compared to simulation results for a set of typical test cases. Fig. 2 shows the results of this comparison for randomly generated design configurations as first test case set (Fig. 2a). This set represents a step towards designing as it includes a set of shapes that are different from the box building in the training data. However, as a constraint of random generation, all storeys of the building have the same shape. The second set is based on a designed building configuration whose geometry and engineering properties are varied by parameters as if it is in a state of preliminary design (Fig. 2d). The complexity of the shape is higher, and the case is more realistic because not all storeys have the same geometry, roofs occur at different levels, and the zone at level two is connected to roofs and a floor slab at the top. This is additional complexity that is not present in the training data and serves to test the ML models for their ability to generalize beyond the training data. For the evaluation, the prediction of component-based ML models and of a monolithic model according to state-of-the-art as baseline method are compared. The state-of-the-art is based on building compactness as performance-characterizing number which currently delivers the best results for monolithic models in representing arbitrary design configurations. The technical details of both models are described in Appendices C and .

The results for the first set consisting of random shapes demonstrate higher precision of the component-based method compared to the state-of-the-art monolithic method. The deviation of ML prediction from simulation results, which act as ground truth, show a mean absolute percentage error (MAPE) of only 3.76% whereas the monolithic baseline model shows a MAPE of 5.88% on average (Fig. 2b). The distribution of errors (Fig. 2c) show a problematic underestimation of energy demand by the monolithic model that is not present for the more precise component-based approach.

The second set of design configurations adds more complexity, as it is usually present in realistic design and engineering cases of buildings. Under these conditions, the advantage of the component-based method against the monolithic method significantly increases. The MAPE of the component-based method is 4.96% whereas the MAPE of the conventional method is 12.72% (Fig. 2e). The error of the conventional model is caused by an even higher underestimation whereas the component-based model has a slight overestimation. In many design and engineering applications, the overestimation is much

less problematic than underestimation. This increase of difference for more complex cases is an indicator that the components show a much better ability to represent design configurations from a domain in general instead of being linked to the behavior observable in the training dataset.

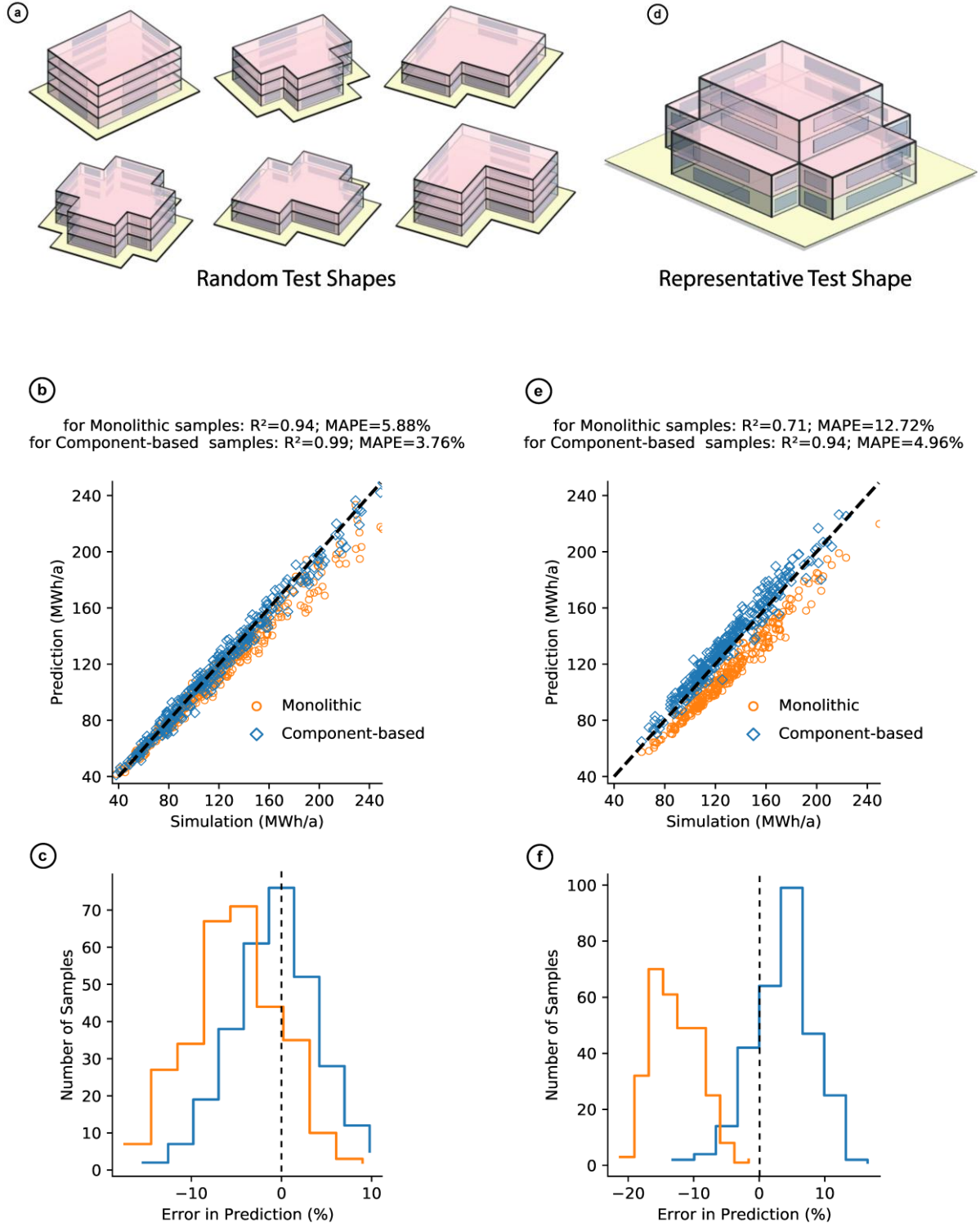


Fig. 2. Prediction accuracy of test cases based on the ML components to evaluate generalization compared with state-of-the-art monolithic ML models. The comparison of ML predictions by the component-based method and state-of-the-art monolithic to ground truth by simulation serves to examine generalization. **(a)–(c):** Comparison of randomly generated shapes with all storey same geometry as in the training data; **(d)–(f):** More complex designed configuration varied by engineering and geometry parameters. This configuration differs from the training data by a roof also at an intermediate level.

In summary, the decomposition allows for extending the application range of the data models beyond training space and, thus, generalization without extrapolation. The scheme to achieve this generalization consists of the extraction of training data from one case, the encapsulation of component behavior as a data-driven model by ML, and the application by composition of data-driven models to the novel structures. This scheme is a form of inductive transfer learning (TL)[29] that is aligned to the engineering reasoning, to the underlying rules and, eventually, to the basic physical laws as a form of domain knowledge. The matching of the structure of the domain knowledge as well as that of probability distributions of features or parameters forms an important condition of the transfer [30]. The component approach provides the basis for this inductive TL. We see it as a special class of inductive TL that extends data information by engineering knowledge consisting of the decomposition and re-composition of the artefact according to paradigm of systems engineering.

A DOMAIN KNOWLEDGE INTEGRATION IN CBML

Component-based ML is a way to align data-driven models with domain knowledge. The taxonomy of von Rueden et al. [31] lists four entities in a prototypical machine learning pipeline to integrate knowledge: training data, hypothesis set, learning algorithm, and final hypothesis. The focus of CBML is the integration of domain knowledge in the hypothesis set by the radical organization of the network architecture according to the domain knowledge and respective structures. In case of the example domain energy-efficient building design, the structure origins from the building systems including its services and constructions. The domain-related model structure enables further connection to domain knowledge in the final hypothesis, i.e., the resulting predictions of CBML, and eventually generates explainability as discussed by [32]. A further source for knowledge embedded in components is the use of dynamic simulation to generate training data. By acquiring and using simulation results that are aligned to the component structure, CBML incorporates domain knowledge embedded in the complex system of the dynamic simulation model and its incorporated differential equations.

B DOMAIN CHARACTERIZATION AND METHOD TRANSFER

To understand the transferability of the approach, a characterization of the case with its basic systems behavior provides a basis. The CBML approach has been demonstrated by prediction data of the dynamic behavior of buildings in terms of energy performance. Underlying energy performance simulation of buildings typically involves a system of coupled partly linear or linearized and partly non-linear ordinary or partial differential equations (ODE/PDE) as well as differential algebraic equations (DAE) [33]. Typically, simulation, such as the software EnergyPlus [34], which has been used for training data generation, performs discretization and applies a set of coupled linear and non-linear solvers to generate point estimates and timeseries results.

In terms of transfer, this system of engineering entities that, on the one hand, rely engineering knowledge in their decomposition and, on the other hand, are described by differential equations with different degree of non-linearity are typical for many engineering applications. Other fields in civil, mechanical, and electrical engineering use similar systems models consisting of a set of differential equations to be solved in simulation for which analogous surrogate models by ML seem feasible. Such examples are systems in electric circuits and respective control and power engineering problems with typically non-linear ODE and DAE [35]. A second example are multibody mechanics that involve ODE and DAE [36]. In contrast, the component-based approach is not directly applicable to such simulations as computation fluid dynamics (CFD) or acoustics, which do work with a node-like system structure but with fields of their key quantities.

III. EXPLAINABILITY IN A COMPONENT-BASED CONTEXT

Using the derived data-driven model and the representative case from the previous section (Fig. 2b), we demonstrate in this section different approaches of explainability enabled by component-based ML. The first subsection deals with intrinsic explainability directly offered by the component interfaces in the

system of the data-driven model. The second subsection deals with sensitivity analysis as a form of engineering interpretation for design space exploration (DSE) locally around the representative case. The third subsection creates a decision tree as explainable surrogate model based on the local DSE data and evaluates this model for engineering rules and their correspondence to domain knowledge of design and engineering.

A ENGINEERING INSIGHTS IN COMPONENT SYSTEMS

A common approach to explain the prediction of DNN is the analysis of the activations and its propagation for a selected prediction case [37]. Layer-wise relevance propagation (LRP)[38] is a method used in image classification. Equivalently to DNN used in image analysis, the CBML structure forms a DNN. In contrast to the monolithic models, the use of components and engineering parameters in between enables direct intrinsic interpretation of the activations as engineering quantities. These quantities enable engineers and designers to understand and check these results in the context of their professional experience.

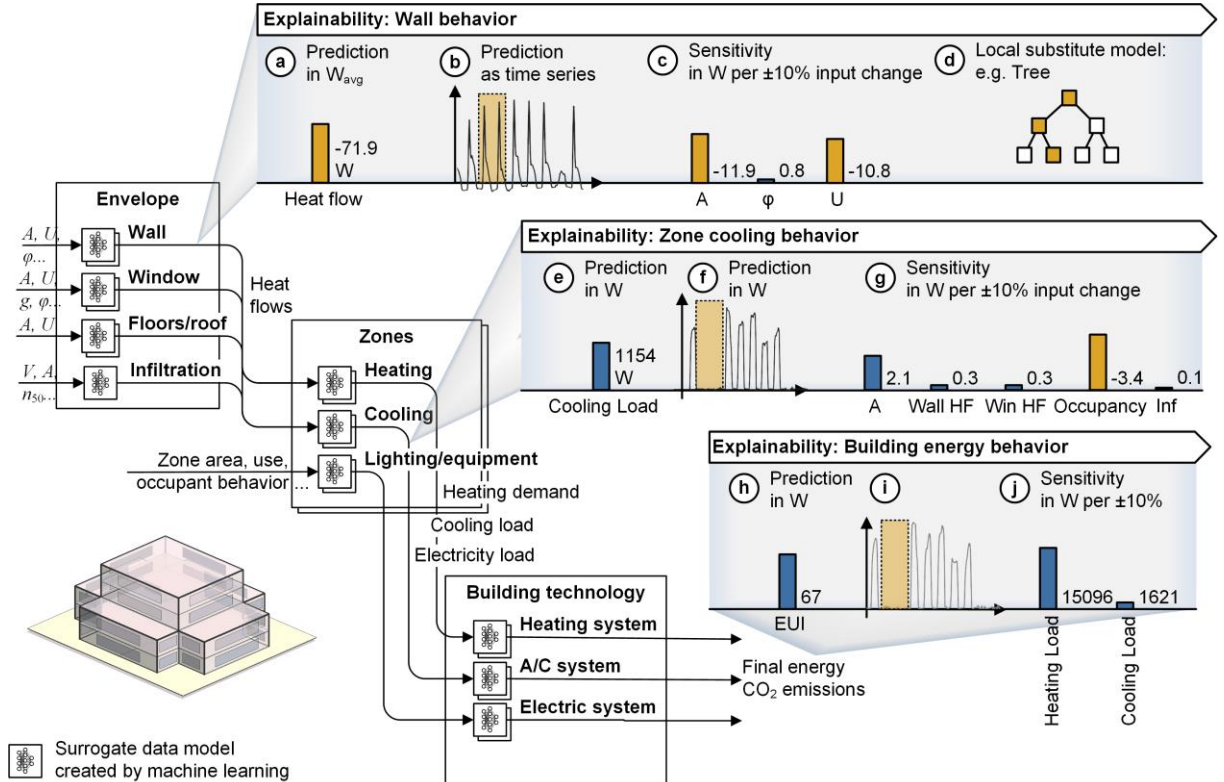


Fig. 3. Accessing information for explainability in a component-based machine learning model. Accessing activations in engineering units between the components provides manifold engineering insights. The analysis of flows in totals (a) (e) (h) and time series (b) (f) (i), sensitivities (c) (g) (j) and extracted rules based on decision trees (d) provides explainability. Humans can interpret results and understand the artefact's behavior.

Figure 3 shows exemplary internal prediction steps such as point estimates (a, e) and time series (b, f) for wall heat flows and zone cooling load. These interim results illustrate how CBML model offers engineering insights. For instance, the time series (b) shows the heat flows through the East walls of the representative testcase building. The morning sun heats up the wall causing the peaks on each of the daily flows whereas the medium level of heat transfer is related to conduction of heat from outside air to indoor space; negative values show heat loss through the walls in the night. Furthermore, the orange dashed box for wall heat flow and cooling load time series (Fig. 3b and f) indicates the weekend. Cooling loads (f) have a high peak after the weekend compared to the Friday before the weekend; this is caused by the heating-up the building while the cooling system is turned off over the weekend. These

observations of activations interpretable as engineering information within the composed DNN system enable domain experts to understand processes, to check results for plausibility, and to evaluate and modify the current design behavior.

B LOCAL MODEL EXPLANATION BY SENSITIVITY ANALYSIS

An alternative approach to examining activations directly is the local variation according to DSE and sensitivity analysis to gain information on reasons for prediction. This approach, which is a traditional engineering method to understand models' behavior, is closely related to local interpretable model explanation (LIME)[39], which is applied to classifiers for explaining results. It belongs to the model-agnostic post-hoc techniques of explainability [20]. From an engineering perspective, a linear local model built on DSE results delivers a regression coefficient that describes sensitivity and enables interpretation of the importance of parameters in the model. Sensitivities for design variables and flow parameters provide valuable insights in the behavior of a specific design configuration. Such information requires two or more evaluations per parameter. An efficient determination is therefore only possible based on data-driven models.

Figure 4 shows selected sensitivities for the representative testcase. First, the matrix shows high sensitivities of the South wall and window heat flow for length and height of the building. A change of these parameters from -10% to +10% leads to about $100 \text{ W}_{\text{avg}}$ additional heat loss but about $300 \text{ W}_{\text{avg}}$ additional heat gains through the windows (Fig. 4a). This tells domain experts that the South windows are worth for looking for heat gains and energy savings. However, to understand the real potential one needs to know whether these heat gains occur in summer or winter. Looking at the g value, also called solar heat gain coefficient, gives an answer (Fig. 4b): A change of the g value from -10% to +10% increases heat gains by $400 \text{ W}_{\text{avg}}$; it reduces heating load by $380 \text{ W}_{\text{avg}}$ and total operational energy by 250 kWh/a . However, it increases cooling loads by $370 \text{ W}_{\text{avg}}$ telling designers and engineers that external shading is a good option. This exemplary interpretation of the behavior of the South windows in the representative case shows how such information provides insights and helps domain experts to draw conclusions for design development. Besides direct engineering reasoning, sensitivities are a means to determine which parameters of a design are important. In early design phases, they provide an indicator which decisions should be made early to reduce the uncertainty in predictions and, thus, offer potential in guiding decision makers through the process [40].

The component-based structure of the model and the calculation of sensitivities makes system analysis and, especially, complexity metrics available [24]. This connects data-driven models to the approach of the design structure matrix (DSM) that deals with the structure of design artefacts, processes and teams and aims at an optimal management of dependencies [41]. As an example of such techniques, Figure 5 shows the sensitivity matrix of key variables and main internal parameters. In the center, the zero-preserving standardized sensitivities are color-coded (a) extending the information partly shown in Figure 4. Analyzing the matrix delivers clusters, such as strong geometric dependencies at the top of the matrix, the window g -value and u -value discussed before, and a cluster of operation linking office hours, heat gain of equipment and light and occupancy to loads and energy demand (last four rows and columns of the matrix). This directs decision makers to parameters that need to be considered simultaneously.

Moreover, summing up columns and rows in the matrix delivers activity and passivity, which are two common complexity metrics of systems. Activity (Fig. 5b) points to variables that have high potential to control the system. In the example, these are variables controlling the building geometry, the passivity (Fig. 5c) points to parameters that have strong reactions and, thus, strongly depend on the configuration of the system. Among these parameters, cooling load is striking, which means the system in its current configuration is relatively sensitive to cooling loads; there is high potential to improve performance by looking at this parameter and its influencers.

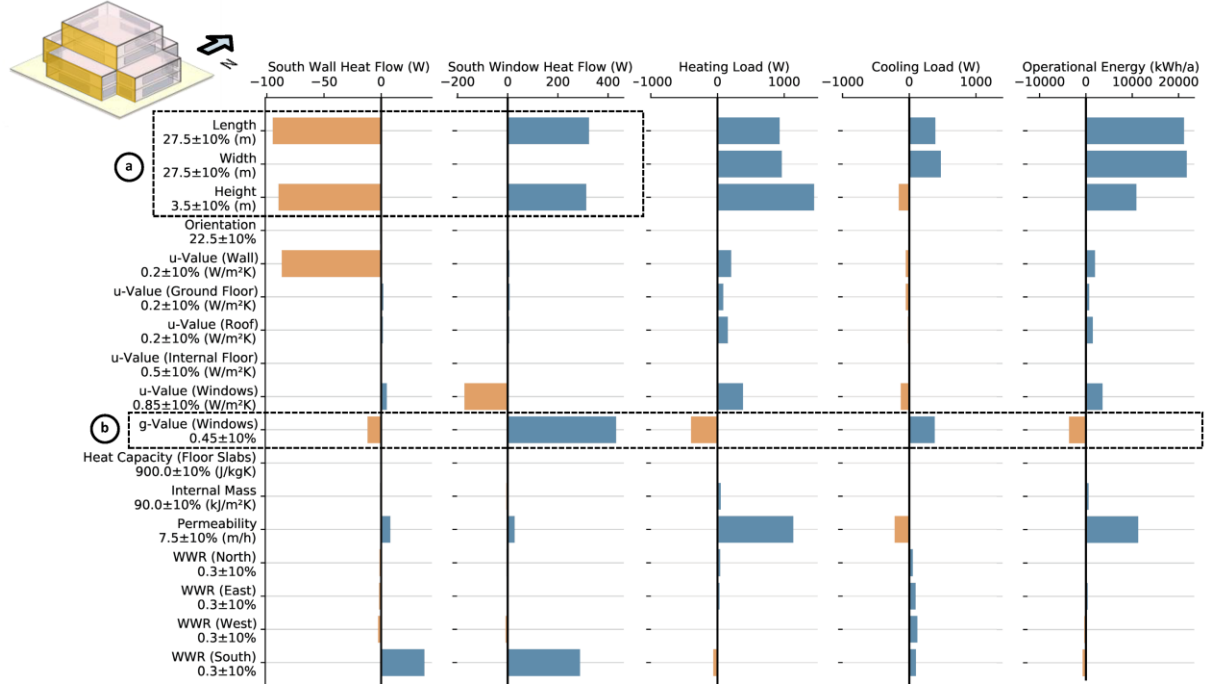


Fig. 4. Selected sensitivities of the representative testcase. The sensitivities provide domain experts identify important variables of a design configuration. (a) A high sensitivity to geometry and higher gains than losses through the South window are visible. (b) The examination of the g-value allows to understand if gains happen in summer or windows.

In sum, the calculation of sensitivities as means to understand dependencies delivers valuable information on the system's structure. This information provides decision makers with understanding which are the key parameters to control system's performance and which parameters and dependencies can be neglected. The use of data-driven models allows for the quick calculation of such information. Furthermore, this information provides a check of plausibility in terms of engineering by comparing dependencies with known engineering equations.

C RULES FROM LOCAL DECISION TREES

Another method to gain insights in reasons for prediction are local surrogate models. In this subsection, decision trees serve as local surrogate model. Trees with low depth allow the extraction of rules that are understandable by engineers and provide further information compared to sensitivities. For the local DSE data, Figure 6 exemplifies such a tree for the windows of the representative building and provides design rules for the current configuration to control the heat flow through the windows. Examining split points allows the derivation of what-if rules. The first split for the configuration is the size of windows (Fig. 6a) telling the decision maker that small windows require different strategies than large ones. The next two splits (b) identify window orientation as the second most important. Focusing on the south windows following the orange prediction path, area and g value, which describes the solar heat gain of windows, are the key variables to control the heat flow at the next levels (c, d). In contrast, the East window splitting also includes the u value, which points to the importance heat conduction for this orientation. The final prediction (e) shows that orientation and g value are the guiding variables for the performance of the South windows telling designers to pay attention to these variables. Furthermore, the upper half of the scatter plots (a, b) provides the information that area and orientation have the highest influence. In particular, increasing area and solar incidence maximize the solar gains directing designers to passive solar building design [42]. Manual studies and extensive sampling for similar climate based on energy simulation performed in other studies confirm the importance of these variables [40], [43].

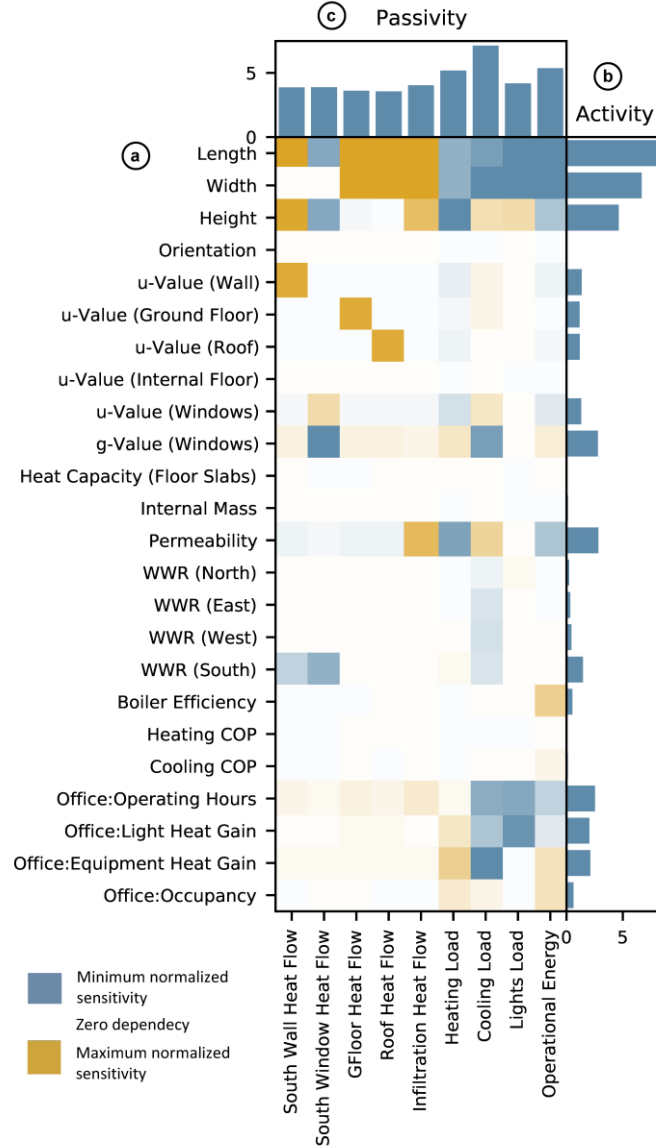


Fig. 5. Sensitivity matrix shows dependencies between key design variables and internal parameters. (a) The per column zero-preserving standardized sensitivities based on linear regression coefficients show the individual dependencies between design variables and internal parameters. (b) The activity sum of absolute sensitivities determines to which extent a variable controls the outcome. (c) The passivity determines to which extent a parameter is controlled by variables.

From the rules of the tree and the underlying data, the application of regression is a method to derive local engineering equations. For instance, a linear regression for the heat flow through large South windows depending on area and g-value (Fig. 6f) allows decision makers not only to derive rules from the tree but also to quantitatively assess the effect of changing window size and solar transmittance on the gains and losses.

IV. DISCUSSION AND CONCLUSIONS

The component-based method of data-driven models offers momentous benefits in engineering design contexts. We have demonstrated that the method provides far better generalization by referring to domain knowledge and structures. Creating data-driven models following decomposition schemes of the domain allows for embedding knowledge and for representing a comprehensive range of configurations compared to limited conventional monolithic data-driven models. Recurring components are the key to predict configurations whose feature structure is not included in the training data and leads to higher accuracy. Especially the two different datasets of the testcases, the randomly created one and

the one intentionally equipped with more complexity that has not been present in the training data show the better ability of the component-based approach to generalize far better beyond training data. It predicts novel unseen cases with roofs at an intermediate level with lower error (MAPE of 4.96% instead of 12.72% for the conventional monolithic model, R^2 of 0.94 instead of 0.71).

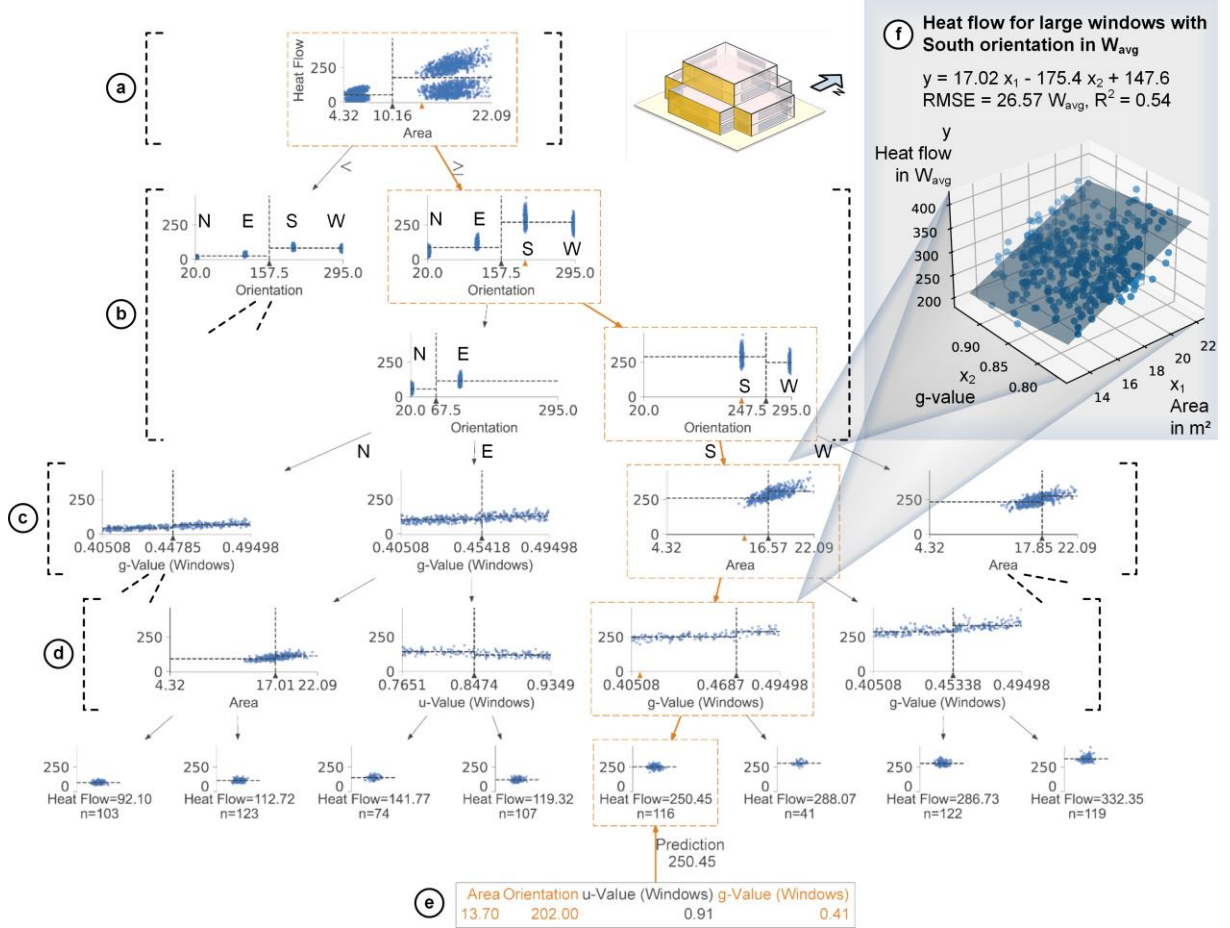


Fig. 6. Decision tree forming a local surrogate model for the windows. Area (a) and orientation (b) are the most important split points. The splitting below (c, d) depends on these variables revealing specific rules for designing windows.

Additionally, by matching similarity in data structure and probability distribution of parameters at component level, predictions for really novel design configurations differing significantly in structure become possible. Especially, the more complex manually designed representative case demonstrated that also adding more complexity in structure and thermal engineering is possible. The observed tendency of the detailed component-based model when leaving range of training data in contrast to the monolithic models that underestimate is a highly interesting characteristic. However, this characteristic needs further observation in different application contexts.

The second advantage of the component-based structure is explainability. The data-driven multi-component model equals an DNN. However, at the interfaces between components, the activations are rescaled to engineering quantities. This enables the direct interpretation of parameters at the interfaces and, thus, internal processes of the engineering artefact, as demonstrated for average and time series flows in energy efficient building design. For design activities, it is highly relevant to answer what-if questions to understand the behavior of the design artefact. Information derived from local sampling allows to generate surrogate models that allow to answer such questions for the specific configuration. As shown, sensitivities provide valuable quantitative information about parameter changes directing designers and engineers to well-performing solutions. Simple trees generated for the local sampling data reveal design rules that are aligned to the specific case. Such rules form a bridge to conventional human

engineering design knowledge and enhance it by offering quantitative case-related support. In the example, the strategy of large windows with a glazing allowing sun to enter the building as well as shading for the summer relates to classical design strategy called solar passive building design that is well known in energy efficient architecture. However, the applicability to the case and the precise configuration require detailed examination. The use of the data-driven models has high potential to assist by specific quantitative reasoning. Using the component-based approach required generalization and explainability of such models are available.

The decomposability determines the realm of applicability of the component-based method. As far as it is possible to break down a model of an artefact to interacting parts, the creation of components is possible. As such an approach is widespread in engineering design—formalized by the method of systems engineering—there is high potential of application and integrating data-driven models with respective design activities in this way. For determining applicability, a further differentiation is important: It is relevant if the models include loops. The demonstrated case relies on a pure hierarchical decomposition without loops allowing prediction in one step. In this way, it is fully compatible to ML software packages. In case of loops, an iterator with a stop criterion is required. This mechanism is a first step towards simulation and points to the integration of data-driven components in simulations, which has also high potential. Alternatively, it is also possible to eliminate loops by surrogates. The time series predictions is such a case that replaces the detailed iterative simulation of dynamic thermal processes and its complex physical models, speeding up predictions and enabling far more predictions. This controlled and validated replacement, which is the key to access the benefits of data-driven models, allows decision makers to explore the design space much better not only leading to improved solutions but also to a deeper understanding of the design's behavior.

In sum, the decomposability of an engineering design in interconnected components according to the paradigm of systems engineering demarcates the applicability of component-based data-driven modelling. If this condition is given, data-driven models structured in this way offer the advantages of a high generalization for engineering design and explainability in form of a good accessibility for engineering interpretation providing engineers with a natural understanding of data-driven predictions. Both, generalization and explainability are vital to develop intelligent assistance based on machine learning that supports designers and engineers in decision making with valuable information to achieve more sustainable artefacts.

APPENDIX

APPENDIX A: DATA GENERATION USING DYNAMIC ENERGY SIMULATION

ML model training and testing requires a large amount of training data covering different design configurations. As it is difficult to collect such examples from real buildings, a common approach is to develop and validate a dynamic simulation model and to use it to generate synthetic data. We developed an EnergyPlus (EP)[34] simulation model for an existing office building in Munich and validated this model against data measured for two years. The building's parameters are listed in Table 1 and floor plan is shown in Figure 7. The measured total of heating and cooling energy demand is 43.97 MWh/a whereas the simulated value is 43.98 MWh/a. The simulated lighting energy demand is 21 MWh/a, for which the real data is not available. The total energy demand corresponds to 54.6 kWh/m²a. The simulation model and measured data is available on Mendeley datasets [44].

Table 1. Parameters of the simulation model for the real building

Parameters	Unit	Value
Floor-to-floor Height	M	3.25
Number of floors	-	3
u-value (Wall)		0.18
u-value (Ground Floor)	W/m ² K	0.19
u-value (Roof)		0.15
u-value (Window)		0.87
g-value		0.35
Heat Capacity (Slab)	J/kgK	800
Permeability	m ³ /m ² h	6
Internal Mass	kJ/m ² K	120
Operating Hours	H	11
Occupant Load	m ² /Person	24
Light Heat Load	W/m ²	6
Equipment Heat Load	W/m ²	12
Heating COP	-	2.8
Cooling COP	-	3.6
Boiler Efficiency		0.95

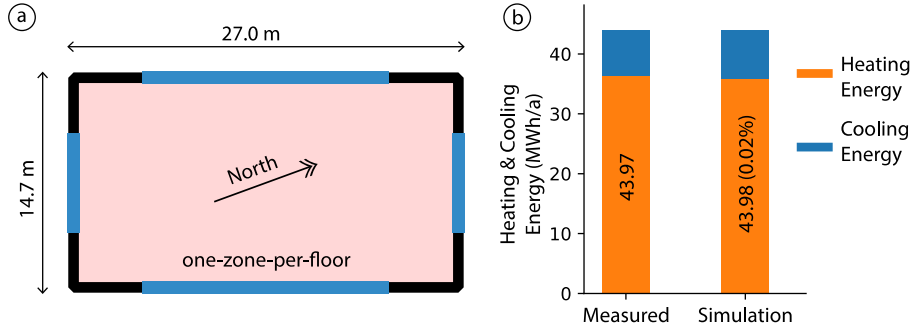


Fig. 7. Comparison of simulated and actual energy consumption. (a) building floor plan (zoning model). (b) measured and simulated heating & cooling energy requirements

Representative key design parameters and their ranges have been selected to generate data covering design configurations. In this selection previous studies and relevant German standards served as reference [45]–[47]. The parameters used in this article are shown in Table 2. These parameters are selected based on their relevance for the design activity at the early design stage as known from previous examination [40].

The design parameters are sampled using Sobol scheme to generate 1000 random samples for training data. For each sample, an EP model is created and simulated. Simulation results collected as training data include average and totals as well as time-series for heat flows, loads, and energy consumption. The training data consists of box-shaped building samples (Fig. 1a), while the test dataset consists of random shapes (Fig. 2a) and a manually designed representative shape (Fig. 2b). Latin hypercube sampling is used to generate 300 random samples for the test dataset. Additional 300 samples are generated for the representative case. The design cases of the test and representative dataset are more complex than the training dataset. This allows for testing the generalizability of CBML approach on complex design cases.

Table 2. Parameters and their ranges for training and test datasets

Parameter	Unit	Min	Max
Length/Width ¹	m	12	30
Ground Floor Area ²	m ²	250	800
Height	m	3	4
Orientation	Degrees	0	90
Number of Floors	-	2	5
u-Value (Wall)		0.15	0.25
u-Value (Ground Floor)		0.15	0.25
u-Value (Roof)	W/m ² K	0.15	0.25
u-Value (Internal Floor)		0.4	0.6
u-Value (Windows)		0.7	1.0
g-Value (Windows)	-	0.3	0.6
Heat Capacity (Slab)	J/m ³ K	800	1000
Internal Mass Heat Capacity	kJ/m ² K	60	120
Permeability	m ³ /m ² h	6	9
WWR ³	-	0.1	0.5
Boiler Efficiency		0.92	0.98
Heating COP	-	2.5	4.5
Cooling COP		2.5	4.5
Operating Hours	h	10	12
Light Heat Gain	W/m ²	6	10
Equipment Heat Gain		10	14
Occupancy	Person/m ²	16	24

¹ Length and Width box-shaped and representative building cases

² Ground Floor Area for random shapes buildings

³ Window-to-wall ratio (WWR) varies independently in each direction

APPENDIX B: MONOLITHIC BASELINE EXPERIMENT

Previously, researchers have proposed monolithic approaches to develop ML-based energy prediction model for different building shapes. This approach uses the parametric building characteristics such as area, u-values, window-to-wall ratios (WWR) etc. and shape factor or relative compactness to represent the shape characteristics. This additional feature represents the volume to surface ratio of the building. Using this approach, this study develops a monolithic ML model as baseline model. The details of input features are provided in Table 3.

Table 3. Input and output of the ML components

ML Component	Input	Output
Monolithic ML model	Floor Area (m ²), Height (m), Number of Floors (-), Relative Compactness (m ³ /m ²), u-Value [Wall, Ground Floor, Roof, Windows] (W/m ² K), g-Value (-), Permeability (m ³ /m ² h), Internal Mass (J/m ² K), WWR [North, East, West, South] (-), Operating Hours (h), Light Heat Gain (W/m ²), Equipment Heat Gain (W/m ²), Occupancy (Person/m ²), Setpoint [Heating, Cooling] (°C), Boiler Efficiency (-), Coefficient of Performance [Heating, Cooling] (-)	Annual Energy Demand (kWh/a)

The baseline monolithic ML model is trained as simple artificial neural network with one input layer, one hidden layer, and one output layer. This study uses L2 regularization and early stopping to prevent overfitting. 20% of the training samples have been used to tune hyperparameters. After a few initial runs, the learning rate has been fixed 0.001, the batch size as one-fifth of the training dataset, activation function as rectified linear unit. A total of sixteen combinations of hyperparameters (four values for number of neurons and four values for the value of regularization coefficient) have been tried and the model with the least validation loss has been kept for further research. Table 4 shows the details of hyperparameters, used for training the monolithic ML model.

Table 4. Details of hyperparameters used for training monolithic ML model

Hyperparameter	Values
Number of Neurons	200, 400, 600, 800
Regularization Coefficient	0.0003, 0.0001, 0.00003, 0.00001
Learning Rate	0.001
Batch Size	One-fifth of sample size
Activation	Rectified Linear Unit (ReLU)

APPENDIX C: COMPONENT-MODEL GENERATION FOR POINT PREDICTIONS

In this approach of CBML, nine ML components are arranged in hierarchical order to predict building energy demand by use of ML for regression. The first level contains five ML components that predict heat flows, corresponding to elements and properties of the building envelope, i.e., wall, window, floor, roof, and infiltration. The second level contains three ML components that predict zone loads related to heating, cooling, and lighting. Finally, the third level has one ML component related to building systems and their properties (heating, cooling and electric) to predict building final energy demand. The input for each ML component is mentioned in Table 5.

Table 5. Input and output of the ML components

ML Component	Input	Output
Wall	Area (m^2), orientation ($^\circ$), u-value (W/m^2K)	
Window	Area (m^2), orientation ($^\circ$), u-value (W/m^2K), g-value (-)	
Floor/ roof	Area (m^2), u-value (W/m^2K), heat capacity (J/kgK)	Heat Flow (W)
Infiltration	Area (m^2), height (m), permeability (m^3/m^2h), heat capacity (J/kgK)	
Zone heating/ cooling load	Area (m^2), [wall/ window/ floor/ roof/ infiltration] heat flow (W), Internal Mass Heat Capacity (kJ/m^2K), [light/ equipment] heat gain (W/m^2), operating hours (h), occupancy (Person/ m^2)	Heating/ cooling Load (W)
Zone lighting load	Area (m^2), light heat gain (W/m^2), operating hours (h), window area (m^2), g-value (-)	Lighting Load (W)
Building energy demand	Boiler efficiency (-), [heating/ cooling] COP (-), [heating/ cooling/ lighting] load (W/m^2)	Annual Energy Demand (kWh/a)

Each ML component has a typical artificial neural network (ANN) architecture. There is one input layer, one hidden layer, and one output layer. During component training, 20% of the training data is kept as validation dataset. After few trial runs, the learning rate has been fixed to 0.001, batch size to one-fifth of the training dataset, and activation function to rectified linear unit (ReLU). The model uses both L2 regularization and early stopping to prevent overfitting. Sixteen different combinations of coefficients for regularization and the number of neurons in the hidden layer have been tested. The best model with the least validation error has been retained for further research.

Table 6. Details of hyperparameters used for training ML components

Hyperparameter	Values
Number of Neurons	200, 400, 600, 800
Regularization Coefficient	0.0003, 0.0001, 0.00003, 0.00001
Learning Rate	0.001
Batch Size	One-fifth of sample size
Activation	Rectified Linear Unit (ReLU)

APPENDIX D: COMPONENT-MODEL GENERATION FOR TIME-SERIES PREDICTIONS

For time series predictors, a component also following the previously used ML-for-regression scheme has been trained and tested with an altered input/output data structure in an additional study [48]. In the data generation process, heat flow, load and energy consumption include the extra dimension time. Furthermore, time series information on the climate is included in training. Feature engineering served to extract and strengthen the periodic characteristics for the model: In our approach, timestamp formatting (year, month, week, day, day of the week, week of the month, hour, etc. plus Boolean value

“is weekday”) has been applied. Another important aspect for the time series prediction is autocorrelation. Feature engineering techniques for shifting, lagging, and window averaging are usually combined in time series data related regression or prediction tasks. In practice, for autocorrelation, input features from n previous states have been used in training phase. Depending on different periodic characteristics, n is set to 3 to 7 days or 12 to 24 hours.

Essentially, the time-series predictor is a regression model, too. The regression algorithm itself has no special requirement on tailoring to fit time series. For the balance of accuracy, difficulty of implementation and interpretability, we used the ensemble method Gradient Boosting Decision Tree (GBDT), which is developed following the concept of boosting [49]. In our implementation, LightGBM [50] using an open-source python library implementation [51] is chosen to fit the regression task.

APPENDIX E: COMPONENT SYSTEM AS A DNN WITH EXPLAINABLE UNITS

Mathematically, the data-driven model based on ANN methods formed by the components constitutes a DNN with one particularity: The component interfaces include scaling and inverse scaling to provide the explainable engineering quantities. In a neural network with the layer function f , the activation function ϕ , and n layers, the function of the neural network for a component g is defined as a nested function:

$$g(\mathbf{x}) = \tau \left(f_{l_{\max},l} \left(\dots f_{2,1 \dots n_l} \left(f_{1,1 \dots n_l} (\sigma(\mathbf{x})) \right) \right) \right)$$

with $f_{l,j}(\mathbf{x}) = \sum_{i=1}^n \mathbf{w}^T \phi(\mathbf{x}) + w_0$; (1)

$$\sigma(\mathbf{x}) = \left. \frac{x - x_{\min}}{x_{\max} - x_{\min}} \right|_{n_{feature}} ; \tau(\mathbf{x}) = \left. x(x_{\max} - x_{\min}) + x_{\min} \right|_{n_{feature}}$$

where σ are τ are the scaling and the inverse scaling functions, \mathbf{x} are the input parameters and \mathbf{w} and w_0 are the learned weightings and offset of the network. As a consequence of the scaling and inverse scaling functions σ are τ , during composition of the data-driven model for prediction, shown in Equation **Error! Bookmark not defined.**, all inputs \mathbf{x} and outputs y of a component are subject to engineering units. By hierarchical nesting of component functions, the DNN is generated that server for prediction:

$$g_{2,1}(\mathbf{x}_{2,1}) = g_{2,1} \left(g_{1,1}(\mathbf{x}_{1,1}), g_{1,2}(\mathbf{x}_{1,2}), \dots, g_{1,n}(\mathbf{x}_{1,n}) \right) \span style="float: right;">(2)$$

In the example on energy performance prediction, the connecting activation between components in this DNN has of W_{avg} and W for the envelope and zone components and $\text{kWh/m}^2\text{a}$ for the building component. In this way, the component interfaces within the DNN link to assessable engineering quantities allowing direct interpretation.

APPENDIX F: SENSITIVITY

The case representing a typical design situation shown in Figures 2b has served to perform local sensitivity analysis. Its parameters are listed in Table 7. A variation of $\pm 5\%$ per design parameter has been considered to calculate local sensitivities \mathbf{S} . These values of \mathbf{S} are obtained by calculating the change in the model response y , when the value of n input parameters \mathbf{x}_S is randomly changed between -5%, 0% and +5%:

$$\mathbf{x}_s = \mathbf{x} \begin{pmatrix} \delta_1 \\ \delta_2 \\ \vdots \\ \delta_n \end{pmatrix} \text{ with } \delta \in [0.95, 1, 1.05]. \quad (3)$$

As components at second and third level rely on intermediate parameters, the direct control of input parameters is not possible. Therefore, coefficients of linear regression model served to determine the sensitivity for these parameters. The values of these coefficients have been adjusted to correspond to the change of $\pm 5\%$ variation in the input \mathbf{x}_s :

$$\mathbf{S} = \text{avg}(f(\mathbf{x}_{+10\%})) - \text{avg}(f(\mathbf{x}_{-10\%})). \quad (4)$$

The sensitivities \mathbf{S} are calculated per flow for each variable in \mathbf{x} . They have the same units as component outputs, i.e. W_{avg} , W , and kWh/m^2a .

Table 7. Parameters for the representative case

Parameter	Unit	Mean
Length/Width	m	27.5
Height	m	3.5
Orientation	Degrees	22.5
Number of Floors	-	4
u-Value (Wall)		0.2
u-Value (Ground Floor)		0.2
u-Value (Roof)	W/m ² K	0.2
u-Value (Internal Floor)		0.5
u-Value (Windows)		0.85
g-Value (Windows)	-	0.45
Heat Capacity (Slab)	J/m ³ K	900
Internal Mass	kJ/m ² K	90
Permeability	m ³ /m ² h	7.5
WWR ¹	-	0.3
Boiler Efficiency		0.95
Heating COP	-	3.5
Cooling COP		3.5
Operating Hours	h	11
Light Heat Gain	W/m ²	8
Equipment Heat Gain	W/m ²	12
Occupancy	Person/m ²	20

APPENDIX G: DECISION TREES

For the local explanation modelling, we chose classification and regression trees (CART)[52] as the surrogate model and visualized the tree nodes with data distributions. As a machine learning model based upon binary trees, the decision tree naturally offers a straightforward rule extraction structure for model interpretation. It learns the relationship by examining and splitting data into binary hierarchical trees of interior nodes and leaf nodes. Each leaf in the decision tree is responsible for making a specific prediction. By exhaustive search, a decision tree carves up the feature space into groups of observations that share similar target values. Each leaf represents one of these groups. The order of the tree splitting is based on the “best” decision attribute for the next node, which is usually evaluated by the information gain (entropy)[53]. As implementations, the decision tree regressor from *scikit-learn* [54] and *dtreeviz* [55] for decision tree visualization have been used. To filter out the irrelevant variation impact from the value range, a min-max scaler transforms each feature individually from the original data to a range between 0 and 1 for splitting. For engineering interpretation, this scale is reverted after tree generation

so that all split points and distribution diagrams include engineering units. For rule extraction in tree interpretation, special attention is paid to the selection of splitting dependent on the previous splitting. If the following split criterion differs in terms of feature selection dependent on a previous split, this is a strong indicator that an engineering rule is underlying, such as different treatment of windows size and façade insulations dependent on orientation in the example.

ACKNOWLEDGEMENTS

The authors acknowledge the support of Deutsche Forschungsgemeinschaft (DFG), Germany, for funding the research through the grant GE1652/3-1/2 within the research unit FOR 2363. The computational resources and services used in this work were provided by the VSC (Flemish Supercomputer Center), funded by the Research Foundation - Flanders (FWO) and the Flemish Government – Department EWI, Belgium.

AUTHOR CONTRIBUTIONS

Philipp Geyer: Conceptualization, Methodology, Software, Validation, Formal analysis, Investigation, Writing - Original Draft, Visualization, Project administration, Funding acquisition

Manav Mahan Singh: Methodology, Software, Formal analysis, Investigation, Writing - Review & Editing + Writing Methodology, Visualization

Xia Chen: Methodology, Software, Formal analysis, Investigation, Writing - Review & Editing + Writing Methodology, Visualization

COMPETING INTERESTS STATEMENT

The authors declare no competing interests.

REFERENCES

- [1] K. Amasyali and N. El-Gohary, “A review of data-driven building energy consumption prediction studies,” *Renewable and Sustainable Energy Reviews*, vol. 81, pp. 1192–1205, Jan. 2018, doi: 10.1016/J.RSER.2017.04.095.
- [2] Y. Wei *et al.*, “A review of data-driven approaches for prediction and classification of building energy consumption,” *Renewable and Sustainable Energy Reviews*, vol. 82, pp. 1027–1047, Feb. 2018, doi: 10.1016/j.rser.2017.09.108.
- [3] T. Østergård, R. L. Jensen, and S. E. Maagaard, “A comparison of six metamodeling techniques applied to building performance simulations,” *Applied Energy*, vol. 211, pp. 89–103, Feb. 2018, doi: 10.1016/j.apenergy.2017.10.102.
- [4] P. Westermann and R. Evins, “Surrogate modelling for sustainable building design – A review,” *Energy and Buildings*, vol. 198, pp. 170–186, 2019, doi: <https://doi.org/10.1016/j.enbuild.2019.05.057>.
- [5] A. Tsanas and A. Xifara, “Accurate quantitative estimation of energy performance of residential buildings using statistical machine learning tools,” *Energy and Buildings*, vol. 49, pp. 560–567, Jun. 2012, doi: 10.1016/j.enbuild.2012.03.003.
- [6] H. Salehi and R. Burgueño, “Emerging artificial intelligence methods in structural engineering,” *Engineering Structures*, vol. 171, pp. 170–189, 2018, doi: <https://doi.org/10.1016/j.engstruct.2018.05.084>.
- [7] H.-J. Rong, G.-B. Huang, N. Sundararajan, and P. Saratchandran, “Online Sequential Fuzzy Extreme Learning Machine for Function Approximation and Classification Problems,” *IEEE Transactions on Systems, Man, and Cybernetics, Part B (Cybernetics)*, vol. 39, no. 4, pp. 1067–1072, Aug. 2009, doi: 10.1109/TSMCB.2008.2010506.
- [8] J. Duan, Y. Ou, J. Hu, Z. Wang, S. Jin, and C. Xu, “Fast and Stable Learning of Dynamical Systems Based on Extreme Learning Machine,” *IEEE Transactions on Systems, Man, and Cybernetics: Systems*, vol. 49, no. 6, pp. 1175–1185, Jun. 2019, doi: 10.1109/TSMC.2017.2705279.
- [9] G. Huang, H. Zhou, X. Ding, and R. Zhang, “Extreme Learning Machine for Regression and Multiclass Classification,” *IEEE Transactions on Systems, Man, and Cybernetics, Part B (Cybernetics)*, vol. 42, no. 2, pp. 513–529, 2012, doi: 10.1109/TSMCB.2011.2168604.
- [10] S. L. Brunton, B. R. Noack, and P. Koumoutsakos, “Machine Learning for Fluid Mechanics,” *Annual Review of Fluid Mechanics*, vol. 52, no. 1, pp. 477–508, 2020, doi: 10.1146/annurev-fluid-010719-060214.
- [11] N. Merchant *et al.*, “The iPlant Collaborative: Cyberinfrastructure for Enabling Data to Discovery for the Life Sciences,” *PLOS Biology*, vol. 14, no. 1, pp. 1–9, 2016, doi: 10.1371/journal.pbio.1002342.
- [12] R. Lokers, R. Knapen, S. Janssen, Y. van Randen, and J. Jansen, “Analysis of Big Data technologies for use in agro-environmental science,” *Environmental Modelling & Software*, vol. 84, pp. 494–504, 2016, doi: <https://doi.org/10.1016/j.envsoft.2016.07.017>.

[13] J. H. Lee, J. Shin, and M. J. Realff, "Machine learning: Overview of the recent progresses and implications for the process systems engineering field," *Computers & Chemical Engineering*, vol. 114, pp. 111–121, 2018, doi: <https://doi.org/10.1016/j.compchemeng.2017.10.008>.

[14] T. Østergård, R. L. Jensen, and S. E. Maagaard, "Early Building Design: Informed decision-making by exploring multidimensional design space using sensitivity analysis," *Energy and Buildings*, vol. 142, pp. 8–22, May 2017, doi: [10.1016/j.enbuild.2017.02.059](https://doi.org/10.1016/j.enbuild.2017.02.059).

[15] J. P. Alves and J. N. Fidalgo, "Classification of Buildings Energetic Performance Using Artificial Immune Algorithms," in *2019 International Conference on Smart Energy Systems and Technologies (SEST)*, Sep. 2019, pp. 1–6. doi: [10.1109/SEST2019.8849140](https://doi.org/10.1109/SEST2019.8849140).

[16] A. Schlueter, P. Geyer, and S. Cisar, "Analysis of georeferenced building data for the identification and evaluation of thermal microgrids," *Proceedings of the IEEE*, vol. 104, no. 4, 2016, doi: [10.1109/JPROC.2016.2526118](https://doi.org/10.1109/JPROC.2016.2526118).

[17] R. Carli, M. Dotoli, R. Pellegrino, and L. Ranieri, "A Decision Making Technique to Optimize a Buildings' Stock Energy Efficiency," *IEEE Transactions on Systems, Man, and Cybernetics: Systems*, vol. 47, no. 5, pp. 794–807, May 2017, doi: [10.1109/TSMC.2016.2521836](https://doi.org/10.1109/TSMC.2016.2521836).

[18] T. Häring, R. Ahmadiahangar, A. Rosin, and H. Biechl, "Machine Learning Approach for Flexibility Characterisation of Residential Space Heating," in *IECON 2021 – 47th Annual Conference of the IEEE Industrial Electronics Society*, Oct. 2021, pp. 1–6. doi: [10.1109/IECON48115.2021.9589216](https://doi.org/10.1109/IECON48115.2021.9589216).

[19] M. Navarro-Cáceres, A. S. Gazafroudi, F. Prieto-Castillo, K. G. Venyagamoorthy, and J. M. Corchado, "Application of artificial immune system to domestic energy management problem," in *2017 IEEE 17th International Conference on Ubiquitous Wireless Broadband (ICUWB)*, Sep. 2017, pp. 1–7. doi: [10.1109/ICUWB.2017.8251010](https://doi.org/10.1109/ICUWB.2017.8251010).

[20] A. B. Arrieta *et al.*, "Explainable Artificial Intelligence (XAI): Concepts, taxonomies, opportunities and challenges toward responsible AI," *Information Fusion*, vol. 58, pp. 82–115, 2020, doi: <https://doi.org/10.1016/j.inffus.2019.12.012>.

[21] S. Singaravel, J. Suykens, H. Janssen, and P. Geyer, "Explainable deep convolutional learning for intuitive model development by non-machine learning domain experts," *Design Science*, vol. 6, p. e23, 2020, doi: [10.1017/dsj.2020.22](https://doi.org/10.1017/dsj.2020.22).

[22] J.-S. S. Chou and D.-K. K. Bui, "Modeling heating and cooling loads by artificial intelligence for energy-efficient building design," *Energy and Buildings*, vol. 82, pp. 437–446, Oct. 2014, doi: [10.1016/j.enbuild.2014.07.036](https://doi.org/10.1016/j.enbuild.2014.07.036).

[23] R. Haberfellner, O. de Weck, E. Fricke, and S. Vössner, "Systems Engineering: Fundamentals and Applications," 2019.

[24] M. Kreimeyer and U. Lindemann, *Complexity metrics in engineering design*. Berlin [u.a.]: Springer, 2011. [Online]. Available: <http://d-nb.info/1010922327/04>

[25] Xia Chen and Philipp Geyer, "Machine assistance: A predictive framework toward dynamic interaction with human decision-making under uncertainty in energy-efficient building design," *submitted*, 2021.

[26] P. Geyer and S. Singaravel, "Component-based machine learning for performance prediction in building design," *Applied Energy*, vol. 228, pp. 1439–1453, Oct. 2018, doi: [10.1016/j.apenergy.2018.07.011](https://doi.org/10.1016/j.apenergy.2018.07.011).

[27] S. Singaravel, J. Suykens, and P. Geyer, "Deep-learning neural-network architectures and methods: Using component-based models in building-design energy prediction," *Advanced Engineering Informatics*, vol. 38, pp. 81–90, Oct. 2018, doi: [10.1016/j.aei.2018.06.004](https://doi.org/10.1016/j.aei.2018.06.004).

[28] R. Sacks, C. Eastman, G. Lee, and P. Teicholz, *BIM handbook: a guide to building information modeling for owners, designers, engineers, contractors, and facility managers*. John Wiley & Sons, 2018.

[29] S. J. Pan and Q. Yang, "A Survey on Transfer Learning," *IEEE Transactions on Knowledge and Data Engineering*, vol. 22, no. 10, pp. 1345–1359, 2010, doi: [10.1109/TKDE.2009.191](https://doi.org/10.1109/TKDE.2009.191).

[30] K. Weiss, T. M. Khoshgoftaar, and D. Wang, "A survey of transfer learning," *Journal of Big Data*, vol. 3, no. 1, p. 9, 2016, doi: [10.1186/s40537-016-0043-6](https://doi.org/10.1186/s40537-016-0043-6).

[31] L. von Rueden *et al.*, "Informed Machine Learning -- A Taxonomy and Survey of Integrating Knowledge into Learning Systems," *IEEE Trans. Knowl. Data Eng.*, pp. 1–1, 2021, doi: [10.1109/TKDE.2021.3079836](https://doi.org/10.1109/TKDE.2021.3079836).

[32] K. Beckh *et al.*, "Explainable Machine Learning with Prior Knowledge: An Overview," *arXiv:2105.10172 [cs]*, May 2021, Accessed: Dec. 29, 2021. [Online]. Available: <http://arxiv.org/abs/2105.10172>

[33] J. Clarke, *Energy Simulation in Building Design*, 2nd Editio. Oxford: Butterworth-Heinemann, 2001. [Online]. Available: <http://www.sciencedirect.com/science/article/pii/B9780750650823500012>

[34] U.S. Department of Energy's (DOE), "EnergyPlus." <https://energyplus.net/> (accessed Jun. 01, 2021).

[35] F. N. Najm, *Circuit Simulation*. John Wiley & Sons, 2010.

[36] J. G. de Jalon and E. Bayo, *Kinematic and Dynamic Simulation of Multibody Systems: The Real-Time Challenge*. Springer Science & Business Media, 2012.

[37] W. Samek and K.-R. Müller, "Towards Explainable Artificial Intelligence," in *Explainable AI: Interpreting, Explaining and Visualizing Deep Learning*, W. Samek, G. Montavon, A. Vedaldi, L. K. Hansen, and K.-R. Müller, Eds. Cham: Springer International Publishing, 2019, pp. 5–22. doi: [10.1007/978-3-030-28954-6_1](https://doi.org/10.1007/978-3-030-28954-6_1).

[38] S. Bach, A. Binder, G. Montavon, F. Klauschen, K.-R. Müller, and W. Samek, "On Pixel-Wise Explanations for Non-Linear Classifier Decisions by Layer-Wise Relevance Propagation," *PLOS ONE*, vol. 10, no. 7, pp. 1–46, 2015, doi: [10.1371/journal.pone.0130140](https://doi.org/10.1371/journal.pone.0130140).

[39] M. T. Ribeiro, S. Singh, and C. Guestrin, "'Why Should I Trust You?': Explaining the Predictions of Any Classifier," in *Proceedings of the 22Nd ACM SIGKDD International Conference on Knowledge Discovery and Data Mining*, New York, NY, USA, 2016, pp. 1135–1144. doi: [10.1145/2939672.2939778](https://doi.org/10.1145/2939672.2939778).

[40] M. M. Singh and P. Geyer, "Information requirements for multi-level-of-development BIM using sensitivity analysis for energy performance," *Advanced Engineering Informatics*, vol. 43, p. 101026, 2020, doi: <https://doi.org/10.1016/j.aei.2019.101026>.

[41] S. Eppinger and T. Browning, *Design structure matrix methods and applications*. Cambridge, Mass: MIT Press, 2012.

[42] J. D. Balcomb, *Passive Solar Buildings*. MIT Press, 1992.

[43] T. Potrč Obrecht, M. Premrov, and V. Žegarac Leskovar, “Influence of the orientation on the optimal glazing size for passive houses in different European climates (for non-cardinal directions),” *Solar Energy*, vol. 189, pp. 15–25, Sep. 2019, doi: 10.1016/j.solener.2019.07.037.

[44] M. M. Singh, “Validation of Early Design Stage EnergyPlus Model for Office Building (one-zone-per-floor model),” Sep. 2021, doi: 10.17632/5kskb6w2s.1.

[45] M. M. Singh, S. Singaravel, R. Klein, and P. Geyer, “Quick energy prediction and comparison of options at the early design stage,” *Advanced Engineering Informatics*, vol. 46, p. 101185, Oct. 2020, doi: 10.1016/j.aei.2020.101185.

[46] Passivhaus Institut, *Passive House requirements*. 2015.

[47] Bundesministerium für Wirtschaft und Energie, “Energy Saving Ordinance (EnEV) 2014, Zweite Verordnung zur Änderung der Energieeinsparverordnung, BGBl I Seite 3951 vom 18.Nov.2013,” 2013. <https://www.bmwi.de/Redaktion/DE/Downloads/Gesetz/zweite-verordnung-zur%20aenderung-der-energieeinsparverordnung.html> (accessed May 21, 2021).

[48] Xia Chen, Manav Mahan Singh, and Philipp Geyer, “Component-based machine learning for predicting representative time-series of energy performance in building design,” presented at the 28th International Workshop on Intelligent Computing in Engineering, Berlin, 2021.

[49] Y. Freund, R. Schapire, and N. Abe, “A short introduction to boosting,” *Journal-Japanese Society For Artificial Intelligence*, vol. 14, no. 771–780, p. 1612, 1999.

[50] Guolin Ke *et al.*, “Lightgbm: A highly efficient gradient boosting decision tree,” *Advances in neural information processing systems*, vol. 30, pp. 3146–3154, 2017.

[51] Guolin Ke and et al., *microsoft/LightGBM*. 2021. Accessed: May 24, 2021. [Online]. Available: <https://github.com/microsoft/LightGBM>

[52] L. Breiman, J. Friedman, C. J. Stone, and R. A. Olshen, *Classification and regression trees*. CRC press, 1984.

[53] B. Hssina, A. Merbouha, H. Ezzikouri, and M. Erritali, “A comparative study of decision tree ID3 and C4. 5,” *International Journal of Advanced Computer Science and Applications*, vol. 4, no. 2, pp. 13–19, 2014.

[54] F. Pedregosa *et al.*, “Scikit-learn: Machine learning in Python,” *the Journal of machine Learning research*, vol. 12, pp. 2825–2830, 2011.

[55] P Terence Parr, Tudor Lapsan, and Prince Grover, “GitHub - parrr/dtreetviz: A python library for decision tree visualization and model interpretation.” <https://github.com/parrr/dtreetviz> (accessed May 24, 2021).